STABILITY ANALYSIS OF SLIP ENERGY RECOVERY INDUCTION MOTOR DRIVE

E. Akpinar E. Ungan

Department of Electrical and Electronics Engineering
Dokuz Eylül University
35160 Buca, Izmir, Turkey

Keywords: Slip energy, stability, linearization.

Abstract: The 4-th order nonlinear transient model of slip energy recovery system (SERS) is linearized around a steady-state operating point using a small signal perturbation technique and the transfer functions which relate the input and output variables are derived. The filter inductance and moment of inertia constant do not have any effect on the operating point of the system at the steady state. The effect of these two parameters on the stability is investigated using linearized model. It is shown that the system is unstable in some range of filter inductance while it is stable throughout its operating range for all values of moment of inertia constant.

1. INTRODUCTION

The slip energy recovery induction motor drive consists of a wound rotor induction motor, three-phase rectifier, three-phase line-commutated inverter, smoothing reactor (filter inductance), and recovery transformer. The conventional form of this drive shown in Figure 1 recovers some part of the energy that would be dissipated in the rotor, and feeds it back to the supply. A three-phase rectifier fed by the rotor converts the rotor voltages at the slip frequency to dc voltage, and a three-phase line commutated inverter is used to convert the zero frequency dc voltage to the ac voltage at the supply frequency. The filter inductance absorbs the difference between the instantaneous inverter input and rectifier output voltages and limits the total harmonic distortion of dc link current. The recovery transformer is necessary if the supply voltage is higher than the rotor terminal voltage.

In the modeling of the SERS, the rectifier input current is assumed to be sinusoidal wave at unity power factor in the synchronously rotating reference frame[1]. This model neglects the overlap angle in the rectifier output voltage as well as the effect of the rectifier and inverter harmonics while they are included into the model in [2]. The average value of the rectifier output voltage, which is approximately proportional to frequency of rotor terminal voltage, is balanced by the inverter input voltage whose average value depends on the inverter firing angle and turns ratio of recovery transformer.

The analysis and stability work done on slip energy recovery system in [4,5] were not correct and resulting voltage equations are invalid [1,3]. Therefore, the comments on the stability region of SERS reported by these papers [4,5] were in mistake. The fourth order non-linear model developed to analyze the SERS at steady state [1] and transient [3] conditions is used here to investigate the stability margin of the drive due to the change of filter inductance and moment of inertia constant which do not change the steady state operating point of the system. The stability margin of the system due to variation of these two parameters is verified by detailed simulation of the system using non-linear transient model.

The paper is organized as follows: Section 2 presents transient model of the SERS while Section 3 has the state space form of linear model. The stability analysis is given in Section 4. Sections 5 and 6 have the results and conclusions, respectively.

2. TRANSIENT MODEL OF SLIP ENERGY RECOVERY SYSTEM

In this section, the transient model of the SERS in the synchronously rotating reference frame is given in per unit. The effect of the complex impedance of the induction motor on the overlap angle in the rectifier output voltage, the effect of the harmonic content of the inverter input voltage and the rectifier output voltage are neglected. The average values of the rectifier output voltage and inverter input voltage are taken into account. The detailed derivation of (1)-(7) can be found in [1,3].

In this model, the q axis of the rotor windings is positioned such that it coincides with the positive peak value of rotor phase a voltage. The peak value of the source voltage in terms of per unit at the inverter side is equal to that value at the infinite bus side.

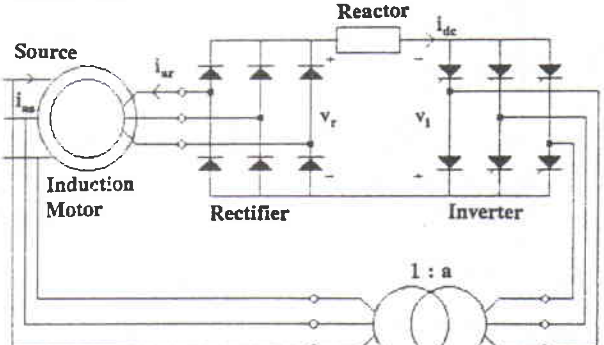

Figure 1. Schematic of a slip energy recovery induction motor drive.

Therefore, the recovery transformer turns ratio naturally disappears in the per unit system.

$$\begin{bmatrix} \frac{di_{qs}}{dt} \\ \frac{di_{ds}}{dt} \\ \frac{di_{qr}}{dt} \end{bmatrix} = A \begin{bmatrix} i_{qs} \\ i_{ds} \\ i_{qr} \end{bmatrix} + B \begin{bmatrix} v_{qs} \\ -v_{ms}\cos\alpha \\ 0 \end{bmatrix} \quad (1)$$

where

$$v_{qs} = \sqrt{v_{ms}^2 - [-x_{ss}i_{qs} + r_s i_{ds} - x_m i_{qr} + m)]^2}$$

$$m = \frac{x_{ss}}{w_b}(\frac{(Sx_m i_{qs} + Sx_{rr}' i_{qr})}{(x_m / w_b)} \quad (2)$$

$$A = -\begin{bmatrix} \frac{x_m}{w_b} & 0 & \frac{x_m}{w_b} \\ \frac{x_m}{w_b} & 0 & \frac{x_{rr}' + X_f'}{w_b} \\ 0 & \frac{x_m}{w_b} & 0 \end{bmatrix}^{-1} \begin{bmatrix} r_s & x_{ss} & 0 \\ 0 & Sx_m & r_r' + R_f' \\ -Sx_m & 0 & -Sx_{rr}' \end{bmatrix} \quad (3)$$

$$B = \begin{bmatrix} \frac{L_4}{L_1L_4 - L_2L_3} & \frac{-L_2}{L_1L_4 - L_2L_3} & 0 \\ 0 & 0 & \frac{1}{L_5} \\ \frac{-L_3}{L_1L_4 - L_2L_3} & \frac{L_1}{L_1L_4 - L_2L_3} & 0 \end{bmatrix} \quad (4)$$

Let

$$A = [a_{ij}]$$
$$B = [b_{ij}] \quad (5)$$

$L_1' = x_{ss} / w_b$, $L_2 = x_m / w_b$, $L_3 = x_m / w_b$, $L_4 = (x_{rr}' + x_f') / w_b$, $L_5 = x_m / w_b$

$$R_f' = (\frac{-\pi^2}{18})r_f, \; X_f' = (\frac{-\pi^2}{18})x_f$$

The slip is given as follows;

$$S = (w_e - w_r) / w_e \quad (6)$$

The per unit electromagnetic torque in the synchronously rotating reference frame is

$$T_e = -x_m i_{ds} i_{qr} \quad (7)$$

The torque balance equation for the mechanical motion can be given as

$$T_e = T_L + 2H \frac{d}{dt}(\frac{w_r}{w_b}) \quad (8)$$

where T_L is the load torque in per unit and H is the inertia constant expressed in seconds [6].

3. STATE-SPACE FORM OF LINEAR MODEL

It can be observed from the nonlinear model (1), there are two inputs of the system that can be varied separately. One is the supply voltage and the other is the firing angle of the recovery inverter. The supply voltage is generally the infinite bus voltage (i.e., its magnitude and frequency is constant). Therefore, this input is assumed to be constant and the firing angle is the only varying parameter. The load torque is treated as the perturbed input. This system has two outputs, namely, the rotor current and rotor speed [3]. The system is linearized around the steady-state operating point on the basis of these two input and two output variables as given below in a compact form.

$$\Delta x = J\Delta x + A_1\Delta u + B_1\Delta T_L$$
$$\Delta y = C\Delta x \quad (9)$$

where C is a constant matrix defined below:

$$C = \begin{bmatrix} 0 & 0 & 1 & 0 \\ 0 & 0 & 0 & -w_s \end{bmatrix}$$

and

$$\Delta x = [\Delta i_{qs} \;\; \Delta i_{ds} \;\; \Delta i_{qr} \;\; \Delta S]^T$$

where Δ x is a perturbation in the state (currents and slip) and Δ u is a perturbation in the input (Cosα). ΔT_L is a perturbation in the load torque and Δ y is a perturbation of the measured outputs, i.e., i_{qr} and w_r.

Let

$$f_1 = \frac{di_{qs}}{dt}, \; f_2 = \frac{di_{ds}}{dt}, \; f_3 = \frac{d_{qr}}{dt}, \; f_4 = \frac{dS}{dt} \quad (10)$$

The jacobian matrix of partial derivatives evaluated around the steady state operating point of SERS is given in (11).

$$J = \begin{bmatrix} \frac{df_1}{di_{qs}} & \frac{df_1}{di_{ds}} & \frac{df_1}{di_{qr}} & \frac{df_1}{dS} \\ \frac{df_2}{di_{qs}} & \frac{df_2}{di_{ds}} & \frac{df_2}{di_{qr}} & \frac{df_1}{dS} \\ \frac{df_3}{di_{qs}} & \frac{df_3}{di_{ds}} & \frac{df_3}{di_{qr}} & \frac{df_3}{dS} \\ \frac{df_4}{di_{qs}} & \frac{df_4}{di_{ds}} & \frac{df_4}{di_{qr}} & \frac{df_4}{dS} \end{bmatrix} \quad (11)$$

Let

$$J = \left[j_{ij}\right]$$

$$A_1 = \begin{bmatrix} \frac{df_1}{du} & \frac{df_2}{du} & \frac{df_3}{du} & \frac{df_4}{du} \end{bmatrix}^T \quad (12)$$

Hence,

$$A_1 = \begin{bmatrix} -b_{12}v_{ms} & -b_{22}v_{ms} & -b_{32}v_{ms} & 0 \end{bmatrix}^T \quad (13)$$

where b_{12}, b_{22}, b_{32} and v_{ms} are the entrees of matrix B defined in (4) and peak value of the source phase voltage in pu respectively.

$$B_1 = \begin{bmatrix} \frac{df_1}{dT_L} & \frac{df_2}{dT_L} & \frac{df_3}{dT_L} & \frac{df_4}{dT_L} \end{bmatrix}^T \quad (14)$$

Hence,

$$B_1 = \begin{bmatrix} 0 & 0 & 0 & \frac{w_b}{2w_s H} \end{bmatrix}^T \quad (15)$$

3.1 Linearized Model Around the Steady-State Operating Point.

The non-linear model of SERS in (1)-(7) is linearized around the steady state operating point using the equations given in (9)-(15). The linear model is used for the system with A 3-phase, 380V, 3.5Kw, 8.1A, 50Hz, 4-pole slip ring induction machine fed by the SERS having the following parameters in per unit [3].

$$r_s = 0.033,\ r_r' = 0.046,\ r_f' = 0.342,\ H = 0.115$$
$$x_{ss} = 0.814,\ x_{rr} = 0.814,\ x_f' = 2.89,\ x_m = 0.738$$

The effective rotor to stator turns ratio is 0.4. The steady state values of the state variables required in the linearized model are obtained for the firing angle (α) of 104.5 degrees and the load torque of 0.185 pu from the solution of equations (1)-(7) using a fourth order Runga-Kutta integration technique.

The elements of the jacobian matrix are obtained after substituting the steady state operating values of state variables and system constants into the equations given in explicit form in [3]. The moment of inertia constant and filter inductance are kept as variables since the effect of them on the stability will be investigated. These elements in terms of x and H are given below:

$$j_{11} = -[11.265 + \frac{1.5904(10^{-2})}{(2.1102.\ x - 1.4119)10^{-3}}]$$

$$j_{12} = -[314.09 + \frac{0.44347}{(2.1102.\ x - 1.4119)10^{-3}} - \frac{0.18154}{(2.5924.\ x - 1.7345)10^{-3}}]$$

$$j_{13} = -[\frac{-0.17195}{(2.5924.\ x - 1.7345)10^{-3}} - 1.1847 - \frac{1.6727(10^{-3})}{(2.1102.\ x - 1.4119)10^{-3}}]$$

$$j_{14} = \frac{0.66392}{(2.5924\ x - 1.7345)10^{-3}}$$

$$j_{21} = 104.67,\ j_{22} = 0,\ j_{23} = 115.45,\ j_{24} = 0$$

$$j_{31} = \frac{2.1551(10^{-2})}{(2.5924\ x - 1.7345)10^{-3}}$$

$$j_{32} = \frac{0.40066}{(2.5924\ x - 1.7345)10^{-3}}$$

$$j_{33} = \frac{-0.19193}{(2.5924.\ x - 1.7345)10^{-3}}$$

$$j_{34} = \frac{-0.73229}{(2.5924.\ x - 1.7345)10^{-3}}$$

$$j_{41} = 0,\ j_{42} = \frac{-7.6017(10^{-2})}{H}$$

$$j_{43} = \frac{0.44982}{H},\ j_{44} = 0$$

where

$$x = x_{rr}' + x_f'(\frac{\pi^2}{18})$$

The transfer functions [7] between the input variable $\text{Cos}\,\alpha$, disturbance input T_L and the output variables, namely, the quadrature axis component of rotor phase current and rotor speed are given in (14)-(17).

$$G_1(s) = \frac{\Delta i_{qr}}{\Delta \text{Cos}\alpha} = [0 \;\; 0 \;\; 1 \;\; 0][sI - J]^{-1} A_1 \quad (14)$$

$$G_2(s) = \frac{\Delta w_r}{\Delta \text{Cos}\alpha} = [0 \;\; 0 \;\; 0 \;\; -w_s][sI - J]^{-1} A_1 \quad (15)$$

$$G_{TL1}(s) = \frac{\Delta i_{qr}}{\Delta T_L} = [0 \;\; 0 \;\; 1 \;\; 0][sI - J]^{-1} B_1 \quad (16)$$

$$G_{TL2}(s) = \frac{\Delta w_r}{\Delta T_L} = [0 \;\; 0 \;\; 0 \;\; -w_s][sI - J]^{-1} B_1 \quad (17)$$

These transfer functions are computed in terms of H and x by using Mathcad package program

4. STABILITY ANALYSIS OF THE SYSTEM

In multi-input multi-output systems, the stability is guaranteed if non of the transfer functions has any pole in the right half plane. The transfer functions given in (14)-(17) have the same denominator which is the determinant of $[sI - J]$. The Rooth-Hurwitz method is applied on this common polynomial in s having two parameters, namely, H and x. This 4-th order polynomial is:

$$\text{Det} = c_4 s^4 + c_3 s^3 + c_2 s^2 + c_1 s + c_0 \quad (18)$$

where coefficients are

$$c_4 = (2.8363Hx^3 - 5.6932Hx^2 + 3.8092Hx - 84.954H)10^{15}$$

$$c_3 = (3.1951Hx^3 + 16.723Hx^2 - 26.669Hx + 9.4004H)10^{16}$$

$$c_2 = (932.47Hx^3 - 1938.4Hx^2 + 1341.6Hx - 309.16H + 3.604x^2 - 4.8226x + 1.6134)10^{17}$$

$$c_1 = (7134.2Hx^2 - 9546.4Hx + 3193.6H + 2.8081x^2 - 3.7578x + 1.2572)10^{18}$$

$$c_0 = (11.762x^2 - 15.739x + 5.2653)10^{21}$$

. The entries in the first column of the Routh array are formed from the coefficients. The entries denoted as F_4, F_3, F_2, F_1 and F_0 are functions of the parameters H and x. They are given in equation (19).

$$\begin{aligned} F_4(H, x) &= c_4 \\ F_3(H, x) &= c_3 \\ F_2(H, x) &= c_2 - \left(\frac{c_4}{c_3}\right)c_1 \\ F_1(H, x) &= c_1 - \left(\frac{c_3}{c_2 - \left(\frac{c_4}{c_3}\right)c_1}\right)c_0 \\ F_0(H, x) &= c_0 \end{aligned} \quad (19)$$

For a given set of H and x values, stability can be checked by evaluating the functions to determine the signs. Any negative sign indicates instability for the particular set. This test is programmed to systematically double scan the H and x in small steps. Appearance of a negative sign at a step following a previous step with all positive signs signals a point on the stability boundary in H, x plane.

5. RESULTS

The transient analysis of the SERS is carried out by using the equations given in (1)-(8) in order to get the steady state values of state variables. These steady state values are not affected by moment of inertia constant and filter reactance if they are chosen in stable region. The reason of this that the derivative of rotor speed with respect to time is zero at steady state and the rate of change of dc link current will be zero while the system is running at steady state [1].

The stability region of the system is obtained by using the equations given in (19). Figure 2 shows that the system is unstable if filter reactance is chosen less than around 0.7 pu. The blackened area is the unstable region of the system. This result has been checked by using the non linear model of the SERS and pole locations of the transfer functions obtained from the linearized model.

While the system is running at steady state (in stable region) with the moment of inertia constant of 0.115 sec, filter inductance of x_f = 2.89 pu and load torque of 0.185 pu, the filter inductance is changed to x_f' = 0.6 pu (this value is predicted to be in unstable region according to figure 2), Figure 3a and 3b show the stator and rotor currents of the motor during this change. It is clear that motor currents are not damped out after this change applied at 2 seconds in time. The rotor current stays in one direction because the diode bridge rectifier does not allow the dc link current to circulate in opposite direction.

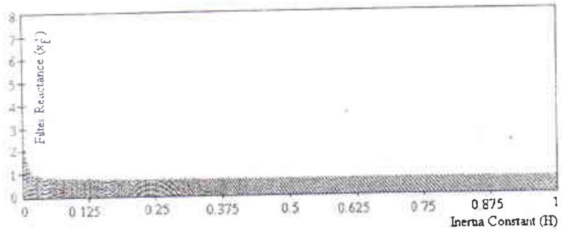

Figure 2. The stability region of the SERS

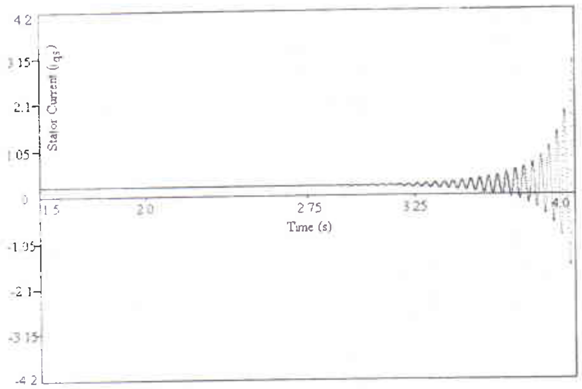

Figure 3a. The quadrature axis stator current in pu.

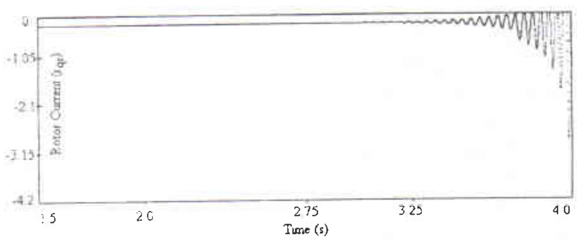

Figure 3b. The quadrature axis rotor current in pu.

If a change on filter inductance is kept in stable region, for instance, it is changed from 2.89 to $x_f' = 1$ pu, the system stays in stable region. This is not shown in a figure because the state variables are still observed around their initial values.

The stability is also checked by computing the roots of polynomial given in (18) using Mathcad. All the poles with negative real part are in stable region for (H=0.115, x_f'=2.89) and (H=0.115, x_f'=1), while some poles have positive real parts in unstable region for (H=0.115, x_f'=0.6).

For H=0.115 and x_f'=2.89, the poles are obtained as follows.

$$s_{1,2} = -5.75 \mp 175.7j$$

$$s_{3,4} = -23.52 \mp 11.06j$$

For H=0.115 and x_f'=1 the poles are obtained as follows.

$$s_{1,2} = -1.5 \mp 169.9j$$

$$s_3 = -16.4, \quad s_4 = -109.8$$

For H=0.115 and x_f'=0.6 the poles are obtained as follows.

$$s_{1,2} = 2.29 \mp 168.5j$$

$$s_3 = -15.5, \quad s_4 = -173.5$$

6. CONCLUSIONS

The Rooth Hurwitz stability technique has been applied on the linearized model of SERS to investigate the stable operating region. The effect of variation of moment of inertia and filter inductance on the stability has been studied. The results shows that there is unstable region of the system as a function of filter inductance. This result is supported by the results of nonlinear model.

REFERENCES

[1] Krause, P. C., Wasynczuk, O., & Hildebrandt, M. S., "Reference Frame Analysis of a Slip Energy Recovery System," *IEEE Transactions on Energy Conversion*, Vol. 3, No. 2, June 1988, pp. 404-408.

[2] Akpinar, E., & Pillay, P., "Modeling and Performance of Slip Energy Recovery Induction Motor Drives," *IEEE Transactions on Energy Conversion*, Vol. 5, No. 1, March 1990, pp. 203-210.

[3] Akpinar, E., Trahan, R. E., Nguyen, A. D., "Modeling and Analysis of Closed-Loop Slip Energy Recovery Induction Motor Drive Using a Linerizatio Technique", *IEEE Transactions on Energy Conversion*, Vol. 8, No. 4, December 1993, pp. 688-697.

[4] Surendran, K., Subrahmanyam, V.,"Stability Analysis of An Induction Motor Drive With a Converter Cascade in the Rotor Circuit Using D-Decomposition Method", International Conference on Electrical Machines, 1986, pp 892-895.

[5] Mittle, V.N., Venkatesan, K., Gupta, S.C.,"Stability Analysis of a Constant Torque Static Slip Power Recovery Drive", *IEEE Transactions on Industry Applications*, Vol. IA-16, No. 1, Jan 1980, pp. 119-126.

[6] Krause, P. C., **Analysis of Electric Machinery**, McGraw-Hill, Inc., 1986.

[7] Dorf, R. C., **Modern Control Systems**, Addison-Wesley Publishing Company, 5th ed., 1989.

[8] Chen, C. T., **Analog and Digital Control System Design**, Saunders College Publishing, 1993.